Impurity peaking in tokamaks

A. Mollén[1], I. Pusztai[1,2], T. Fülöp[1], S. Moradi[1], M. L. Reinke[2], Ye. Kazakov[3]

[1] *Department of Applied Physics, Nuclear Engineering, Chalmers University of Technology and Euratom-VR Association, Göteborg, Sweden*

[2] *Plasma Science and Fusion Center, Massachusetts Institute of Technology, Cambridge MA, USA*

[3] *LPP-ERM/KMS Association "Euratom-Belgian State", TEC Partner, Brussels, Belgium*

Introduction To avoid large radiation losses and plasma dilution, impurity accumulation in the plasma core should be kept at minimum. In the present work we investigate cross-field transport of high-Z impurities, through gyrokinetic modeling and simulations using the GYRO code [1]. Experimentally, the application of radio frequency heating has been shown to give a flattening effect on impurity density profiles in the core. Here we analyze an experimental Ion Temperature Gradient (ITG) mode dominated case from a hydrogen minority Ion Cyclotron Resonance Heated (ICRH) Alcator C-Mod discharge. In previous studies, ICRH has been found to give rise to a poloidally asymmetrically distributed impurity species [2, 3], and a theoretical model for its impact on cross-field impurity transport has been presented [4, 5, 6]. While earlier studies have been limited to theoretical cases, here we apply the model to experimental data. The strength of the poloidal asymmetry is estimated, and the zero-flux impurity density gradient (peaking factor) is calculated and compared to the symmetric case.

Model A semi-analytical linear gyrokinetic model for the zero flux density gradient of high-Z impurities present in trace quantities is introduced in [5], where the effect of a poloidally varying, non-fluctuating electrostatic potential ϕ_E is included. In [6] this model is applied to Trapped Electron Modes (TEM), and demonstrates the ability to reproduce trends of nonlinear GYRO simulations in the poloidally symmetric case. Furthermore a significant reduction of the impurity peaking is found in the poloidally asymmetric case, where the key parameters are the asymmetry strength κ and the magnetic shear s.

We focus on poloidal asymmetries due to poloidal electric fields and neglect effects caused by a radial electric field, such as the centrifugal force arising from toroidal rotation. The poloidally varying potential is assumed to be weak in the sense that $e\Delta\phi_E/T_\alpha \ll 1$ (where T_α is the temperature of species α). This justifies the use of GYRO simulations neglecting poloidal asymmetries to obtain linear mode characteristics, since the effect of poloidal asymmetries on the main species can be neglected. By requiring $Z \gg 1$ however, $Ze\Delta\phi_E/T_z \sim \mathcal{O}(1)$ and the impurities can be poloidally asymmetrically distributed. Hence their $\mathbf{E}\times\mathbf{B}$ drift in the poloidally varying electrostatic potential ϕ_E is not negligible. The model used for the equilibrium electrostatic

potential is given by Eq. (11) in [4]

$$Ze\phi_E/T_z = -\kappa\cos\left(\theta-\theta_0\right), \tag{1}$$

where θ_0 represents the angular position where the impurity density has its maximum and κ sets the strength of the poloidal asymmetry. For experimentally observed low-field-side ICRH driven asymmetries, $\theta_0 = \pi$.

To find the impurity peaking factor, a/L_{nz}^0, we use the model presented in [5] where the peaking factor is given by Eq. (8), here we rewrite it as

$$\frac{a}{L_{nz}^0} = 2\frac{a}{R_0}\langle\mathcal{D}\rangle_\phi + \frac{a}{r}s\kappa\langle\theta\sin(\theta-\theta_0)\rangle_\phi - \frac{2a^2}{(qR_0)^2k_\theta\rho_s}\frac{Zm_i}{m_z}\frac{c_s}{a}\frac{\omega_r}{\omega_r^2+\gamma^2}\left\langle\left|\frac{\partial\phi}{\partial\theta}\right|^2/\left|\phi\right|^2\right\rangle_\phi . \tag{2}$$

ϕ is the perturbed electrostatic potential and $\omega = \omega_r + i\gamma$ the mode eigenvalue, a is the outermost minor radius, r the minor radius of the analyzed flux surface, R_0 the major radius, q the safety factor, $s = (r/q)(dq/dr)$ the magnetic shear, k_θ the poloidal wave number, $c_s = (T_e/m_i)^{1/2}$ the ion sound speed and ρ_s the ion sound Larmor radius. Furthermore $\mathcal{D}(\theta) = \cos\theta + s\theta\sin\theta$ and $\langle\ldots\rangle_\phi = \langle\ldots\mathcal{N}|\phi|^2\rangle/\langle\mathcal{N}|\phi|^2\rangle$ with $\mathcal{N} \equiv \exp\left[-Ze\phi_E/T_z\right]$, and $\langle\ldots\rangle = (1/2\pi)\int_{-\pi}^{\pi}(\ldots)\,d\theta$ denotes the flux surface average. We refer to [5] for details of the model. Note that up to $\mathcal{O}(Z^{-1})$, both finite Larmor radius (FLR) effects and the effects of collisions do not appear. Furthermore we see that a/L_{nz}^0 consists of three terms: the first term of Eq. (2) represents the contribution from magnetic drifts, the second term stems from the $\mathbf{E}\times\mathbf{B}$ drift and is only non-zero in the presence of a poloidally varying potential, the last term arises because of the impurity parallel dynamics and is positive for ITG modes but negative for TEMs.

Alcator C-Mod minority ICRH discharge As a reference, we analyze an Alcator C-Mod deuterium discharge, described in [2], where ICRH was applied with the resonance layer at the low-field-side, $r_c/a = 0.47$, using hydrogen minority scheme. The hydrogen minority concentration at the analyzed flux surface is estimated to be $n_{H0}/n_{e0} = 0.04$, the ICRH resonant magnetic field strength is $b_c = B_c/B_0 = 0.87$ and we assume $T_z = T_i$ and no rotation. The analyzed impurity species in the discharge is partially ionized molybdenum ($^{96}_{42}\mathrm{Mo}$) with $Z = 32$, characteristic of this range of T_e. The molybdenum concentration in ICRF heated shots is estimated to be $n_z/n_e = 10^{-4} - 10^{-3}$ and we assume $n_{z0}/n_{e0} = 2\cdot10^{-4}$.

The asymmetry strength κ is found from Eqs. (10) and (12) of [4], assuming circular flux surfaces (the experimental elongation at the analyzed flux surface is 1.27)

$$\kappa = \frac{Z(n_{H0}/n_{e0})\,k}{(T_z/T_i)(n_{i0}/n_{e0}) + (T_z/T_e) + (n_{z0}Z^2/n_{e0})}, \tag{3}$$

$$k = \frac{\epsilon\, b_c(\alpha_T - 1)}{b_c + \alpha_T(1-b_c)}, \tag{4}$$

where $\alpha_T = T_\perp/T_\parallel$ is the minority temperature anisotropy, found using TRANSP, and $\epsilon = r/R_0$ the inverse aspect ratio. As shown in Fig. 1 the largest asymmetry is found at $r/a = 0.41$ with $\alpha_T = 5.4$ and $\kappa = 0.21$, consequently we will analyze this radial location. Experimental values at $r/a = 0.41$ are $R_0/a = 3.2$, $s = 0.43$, $q = 1.07$, $T_i/T_e = 0.80$, $a/L_{Te} = 1.81$, $a/L_{Ti} = 1.56$, $a/L_n = 0.60$ and $\hat{\nu}_{ei} = 0.065\ c_s/a$.

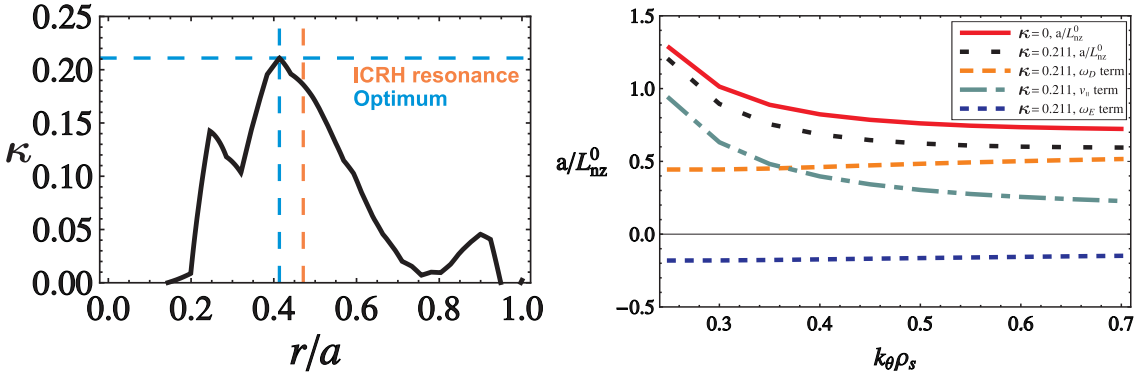

Figure 1: Asymmetry strength κ as functions of r/a (left), and Mo^{32+} peaking factor as function of $k_\theta\rho_s$ for the symmetric ($\kappa = 0$) and asymmetric ($\kappa = 0.21$) cases (right). Also shown are the contributions to the peaking from the three separate terms in Eq. 2: magnetic drifts (ω_D term), $\mathbf{E}\times\mathbf{B}$ drift (ω_E term) and parallel dynamics ($v_\parallel$ term).

A 2D map of the linear mode eigenvalues in $r/a - k_\theta\rho_s$ space for this discharge, obtained with the eigenvalue solver in GYRO, is illustrated in Fig. 2. At the studied flux surface, $r/a = 0.41$, the plasma is ITG dominated and this branch is traced over the radial domain. Note however that, besides from subdominant modes, there could be another mode that even dominates at another radial location.

The Mo^{32+} peaking factor as function of $k_\theta\rho_s$ is shown in Fig. 1. To choose a relevant single mode, we estimate the relative magnitude of the quasilinear fluxes from the quantity $\left[\gamma/\left\langle k_\perp^2\right\rangle\right]_{k_\theta}$,with $\left\langle k_\perp^2\right\rangle = k_\theta^2\left(1 + s^2\left\langle\theta^2\right\rangle\right)$ and $\left\langle\theta^2\right\rangle = \int\theta^2\left|\phi_{k_\theta}\right|^2 d\theta/\int\left|\phi_{k_\theta}\right|^2 d\theta$ from the theory presented in [7], by performing linear GYRO simulations. The poloidal wave number yielding the largest value is $k_\theta\rho_s = 0.35$, with the linear growth rate $\gamma = 0.063\ c_s/a$ and mode frequency $\omega_r = -0.14\ c_s/a$ (ω_r is negative for modes propagating to the ion diamagnetic direction according to GYRO conventions).

From Eq. 2 the molybdenum peaking factor is found to decrease from $a/L_{nz}^0 = 0.89$ in the symmetric case ($\kappa = 0$) to $a/L_{nz}^0 = 0.76$ in the asymmetric case ($\kappa = 0.21$). The contribution from the $\mathbf{E}\times\mathbf{B}$ term is -0.18 in the asymmetric case, but there is a slight increase in the term coming from parallel compressibility between the symmetric and asymmetric cases which

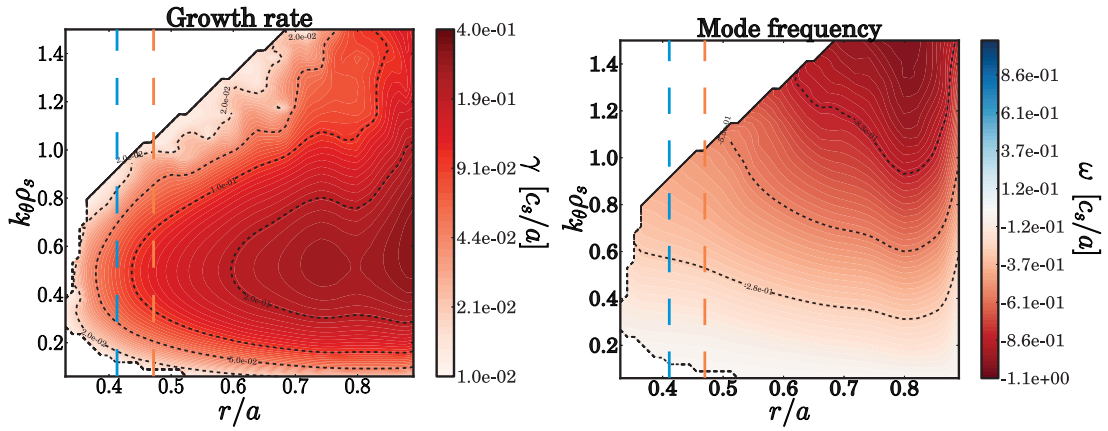

Figure 2: 2D map of linear growth rate γ (left) and real mode frequency ω_r (right) as functions of r/a and $k_\theta\rho_s$ for the ITG branch which is dominant at $r/a = 0.41$. Blue dashed line marks $r/a = 0.41$ where the maximum asymmetry is located, orange dashed line marks $r/a = 0.47$ where the ICRH resonance is located.

counteracts the reduction of the peaking factor.

Conclusions A small reduction in molybdenum peaking is predicted from the poloidally varying non-fluctuating electrostatic potential, which arise due to hydrogen minority ICRH in the analyzed Alcator C-Mod discharge. The reduction is not as large as found in earlier theoretical work [4, 5, 6], which is expected, due to the fact that the magnetic shear is not very large and at the studied flux surface the plasma is ITG dominated. The magnetic shear has previously been found to be a key parameter in determining the magnitude of the reduction and it is relatively moderate at the studied flux surface, $s = 0.43$. Also, TEM dominated scenarios have previously been found to lead to reduced impurity peaking due to the contribution from parallel compressibility. It is possible that subdominant modes play an important role at the studied flux surface. The role of these can be revealed by a nonlinear analysis, which is among our future goals.

References

[1] J. Candy and R. E. Waltz, *J. Comput. Phys.* **186**, 545 (2003).
[2] M. L. Reinke, I. H. Hutchinson, et al, *Plasma Phys. Control. Fusion* **54**, 045004 (2012).
[3] Ye. O. Kazakov, I. Pusztai, et al, *Plasma Phys. Control. Fusion* **54**, 105010 (2012).
[4] A. Mollén, I. Pusztai, et al, Phys. Plasmas **19**, 052307 (2012).
[5] I. Pusztai, A. Mollén, et al, *Plasma Phys. Control. Fusion* **55** (2013) 074012.
[6] A. Mollén, I. Pusztai, et al, Phys. Plasmas **20**, 032310 (2013).
[7] T. Dannert and F. Jenko, *Phys. Plasmas* **12**, 072309 (2005).

Acknowledgments Experiments used in this work supported by US DoE contracts DE-FC02-99ER54512. This work was funded by the European Communities under Association Contract between EURATOM and Vetenskapsrådet.